J|A|C|S COMMUNICATIONS

Published on Web 09/25/2009

Electrochemical Charging of Single Gold Nanorods

Carolina Novo, Alison M. Funston, Ann K. Gooding, and Paul Mulvaney*

School of Chemistry and Bio21 Institute, University of Melbourne, Parkville, VIC, 3010, Australia

Received June 25, 2009; E-mail: mulvaney@unimelb.edu.au

Metal nanocrystals are commonly used to catalyze important chemical reactions such as water splitting and CO oxidation.[1] While it is expected that crystal morphology will be important, only recently has it become possible to synthesize different-shaped metal nanocrystals, enabling the effects of size and shape to be explored systematically. In particular, facets and apexes on metal nanocrystal surfaces provide "hot spots", where the electric field is greatly enhanced. This local field will lead to different rates of electron transfer over the nanocrystal surface. Consequently, the rates of electrochemical reactions on metal nanocrystals will be strongly dependent on the particle morphology.

Current models for redox reactions on metal nanocrystals are based on the microelectrode model introduced by Henglein and colleagues.[2] Bard and colleagues subsequently formulated a general, mixed-potential model to account for redox catalysis on small metal nanocrystals in aqueous solution,[3] and Spiro and co-workers have examined many aspects of this model in detail.[4] More recently, electron transfer between electrodes and ensembles of ultrasmall gold nanoparticles has been studied by Murray and colleagues using cyclic voltammetry, leading to the discovery of quantized charging of metal nanocrystals.[5] However, all the studies to date have been restricted to measurements of ensemble averaged rate constants. This masks the important role of the shape and size of the nanocrystals on the rates of electrochemical reactions. A key challenge is therefore to carry out electrochemistry on single metal nanocrystals.

One possible approach is to use surface plasmon spectroscopy. Spatial confinement of conduction electrons in small gold, silver, and copper particles leads to absorption and scattering resonances, whose energies are altered by changes in electron density. This enables electron-transfer reactions to be observed spectroscopically and with unprecedented sensitivity.[6] We report here that the surface plasmon resonance of a single gold nanocrystal can be reversibly and rapidly tuned by tens of nanometers electrochemically. The spectral shifts are more sensitive for elongated morphologies such as rods and lead to color changes perceptible by eye.

To measure these surface plasmon shifts, we have used dark-field microscopy to study the scattered light from single gold nanocrystals of different morphologies. This technique was pioneered by Klar et al.[7] and Schultz et al.,[8] and enables the spectra of the light scattered by a single nanoparticle to be measured routinely. We have modified this technique to enable electrochemical processes to be studied simultaneously. The gold nanorods used in our experiments were synthesized by standard protocols.[9] Electron micrographs and spectra of the rod ensembles are presented in the Supporting Information. The rods had aspect ratios that varied between 2.75 and 4. Indium-tin-oxide (ITO)-coated glass slides were used as a substrate. Markers were etched using a focused ion beam (FIB) as displayed in Figure 1C, enabling the rods to be imaged in the scanning electron microscope (SEM) before and after experiments and their spectra to be collected.[10] By recording the exact aspect ratio of the rods used in each experiment, the effects of sample polydispersity were avoided. The spectra were measured in a dark-field setup; the light scattered by each individual rod was passed through a grating to a thermoelectrically cooled charge-coupled device camera (the setup used, schematically displayed in Figure 1A, is described elsewhere[10]). Spectra could be collected within 15 s, though for accurate determination of the peak wavelength, spectra were collected for up to 60 s.

To modulate the electron density on the gold nanorods, a thin electrochemical cell (thickness 5 mm) was developed for use under dark-field illumination. The cell, depicted in Figure 1B, is composed of a steel cage and a Teflon ring. Through the ring, a Pt and a Ag wire contact the electrolyte (a 0.1 M KCl solution) and function as counter and quasi-reference electrodes, respectively ($E^\circ = +0.25$ V for ferrocyanide ion vs Ag quasi-reference). Another Ag wire connects the particle-containing ITO-coated slide, the working electrode, to the potentiostat. The advantage of doing the experiments in fluids is that the double-layer capacitance of the particle is almost two orders of magnitude higher than that in air, due to the higher dielectric constant of water and the double layer screening by counterions (see Supporting Information Figure S3). This leads to much larger spectral shifts than are achievable in air.

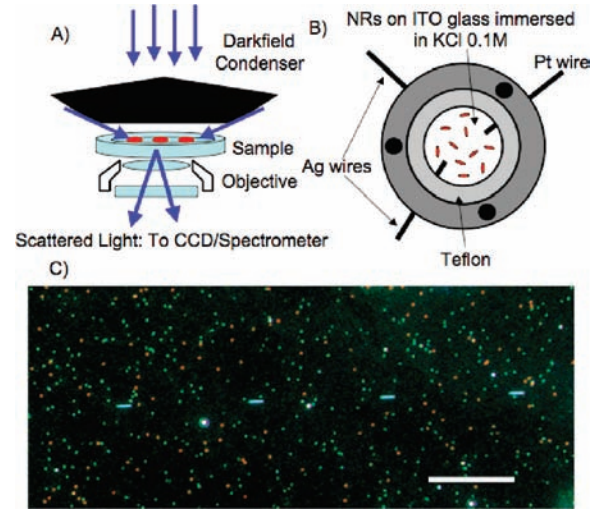

Figure 1. (A) Dark-field microscope with dark-field condenser, objective, CCD camera, and spectrometer. (B) Cell for electrochemical charging under the dark-field microscope, comprising a steel shell with two Ag wires (one contacting the ITO to provide a working electrode, the other a quasi-reference) and an auxiliary Pt electrode. (C) Dark field image of gold nanoparticles deposited onto an ITO-coated glass slide with FIB landmark etchings, scale bar = 40 μm.

When the potential applied to the ITO electrode was changed from 0 V to −0.6 V, only weak spectral shifts were observed, while damage to the ITO substrate was seen when potentials more

10.1021/ja905216h CCC: $40.75

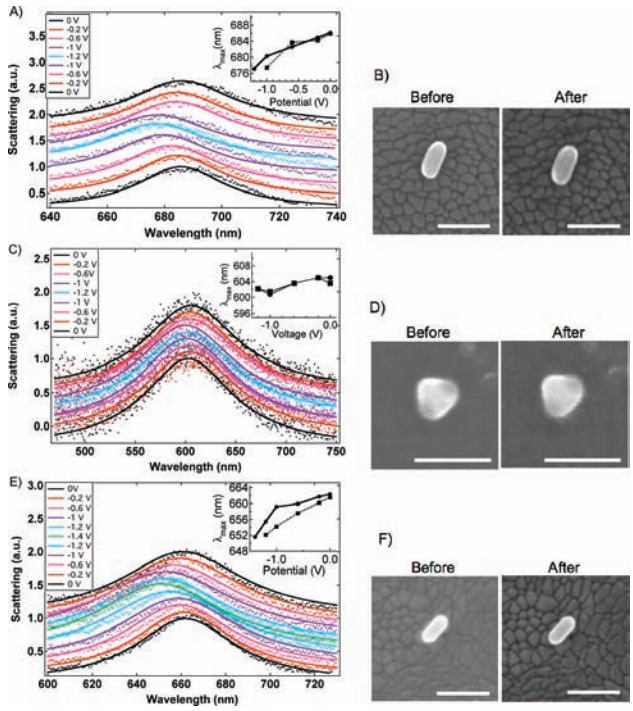

Figure 2. Normalized scattering spectra of gold nanoparticles at potentials varying from 0 V to (A and C) −1.2 V and (E) −1.4 V and back to 0 V. Full lines are Lorentzian fits to the spectra, which are offset for clarity. Insets are plots of λ_{max} vs potential. (E), (D), and (F) are SEM images of the particles in (A), (C), and (E), respectively, before and after the charging; the granular structure is the ITO. Scale bars = 100 nm.

negative than −1.4 V were applied for extended periods of time. However, clear blue shifts were evident for applied potentials ranging from −0.6 to −1.4 V, as shown in Figure 2. Control experiments (Figure S2) show that there are no significant shifts in single-particle spectra in the absence of cathodic charging, and therefore the shifts are not due to heating effects or slow drift in the particle spectra on the time scale of these experiments. The experimentally measured peak shifts were substantially larger than the error in the peak position determined by fitting the spectra to Lorentzian functions, which was estimated to be ±1 nm.

For example, for an applied voltage of −1.4 V, a spectral blue shift of 11 nm was observed for the particle in the SEM images in Figure 2F, while, for an applied voltage of −1.2 V, a shift of 9 nm was observed for the particle in Figure 2B. The surface plasmon band shifts, caused by the electron injection, were largest for gold nanorods. For other morphologies, such as small gold spheres and the small trigonal prism (shown in Figure 2D and analyzed in Figure 2C), both of which have a lower radius of curvature at the tips than the rods, much smaller shifts were recorded at each applied potential.

In the insets to Figure 2, the blue shift is plotted as a function of the applied voltage. A reasonably linear dependence on the applied voltage is observed, though the shift does appear to become stronger at more negative potentials. Upon reversal of the bias, from a large negative potential back to 0 V, the surface plasmon band red-shifted back to the original peak wavelength. The recovery of the initial surface plasmon resonance occurred within the 60 s time resolution with which we could accurately record the peak position. This indicates that electron injection is reversible and that there is facile electron transfer between the particles and the ITO substrate.

Changes in roughness are often observed during electrochemical cycling of smooth metal electrodes, while chemical reactions at the surface of gold rods have also been found to lead to irreversible shape changes.[11] However, the electron micrographs of the rods taken before and after electrochemical cycling (Figure 2) demonstrate that there is no significant change in particle morphology induced by the changes in electron density at the potentials applied. Furthermore, in these experiments the most negative applied potential was −1.4 V, which resulted in a blue shift of 11 nm. From the change in applied potential and the calculated electron density change, we can estimate the double layer capacitance of the gold rods using $C = d\sigma/dV$. This yields 150 μF/cm^2 (see Supporting Information), in reasonable agreement with bulk electrode measurements.[12]

The color changes induced by cathodic charging are substantial and may be observed by eye during the experiments. Typical images, displayed in Figure 3, show clear color changes due to blue shifts in the surface plasmon resonance caused by electron injection into the particles. The rods scatter red light, and this shifts first to orange and then to yellow-orange when a negative bias is applied. The particles scattering green light are spheres or small prisms. They appear to change slightly to blue-green at high cathodic potentials.

To quantify these effects, we note that the bulk plasma wavelength for gold, λ_p, is 131 nm[13] and is a function of only the electron density, N, and the effective mass of electrons, m, in the material, according to eq 1. Combining this equation with the condition for resonance of an anisotropic metal particle within the dipole approximation,[13] it has been shown that the surface plasmon resonance shift depends on the electron density according to eq 2:[14]

$$\lambda_p = \frac{2\pi c}{\omega_p} = \sqrt{\frac{4\pi^2 c^2 m \varepsilon_0}{Ne^2}} \quad (1)$$

$$\Delta\lambda = -\frac{\Delta N}{2N}\lambda_p \sqrt{\varepsilon_\infty + \left(\frac{1-L}{L}\right)\varepsilon_m} \quad (2)$$

In these equations, N is the electron density in the uncharged gold nanorod, ϵ_∞ is the high frequency contribution to the metal dielectric function (12.2 for gold[13]), ϵ_m is the dielectric constant of the medium, ϵ_o the vacuum permittivity, and L the particle shape factor.[13] If the electron density changes to $N + \Delta N$, the bulk plasma frequency is altered correspondingly through eq 1 and also, therefore, the dielectric properties of the gold. Figure 4A shows calculated spectra of a charged rod using eq 3 with an aspect ratio corresponding to the rod in Figure 2F. For this rod, some 85 000 electrons (see Supporting Information) must be injected to account for the blue shift of 11 nm (cathodic potential of −1.4 V).

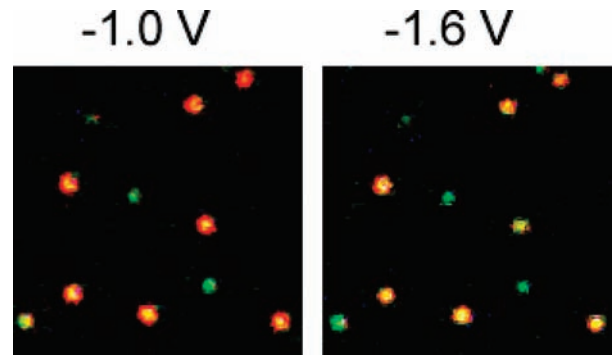

Figure 3. Color images of gold nanorods (red) and spheres or trigonal prisms (green) at applied potentials of −1 V and −1.6 V.

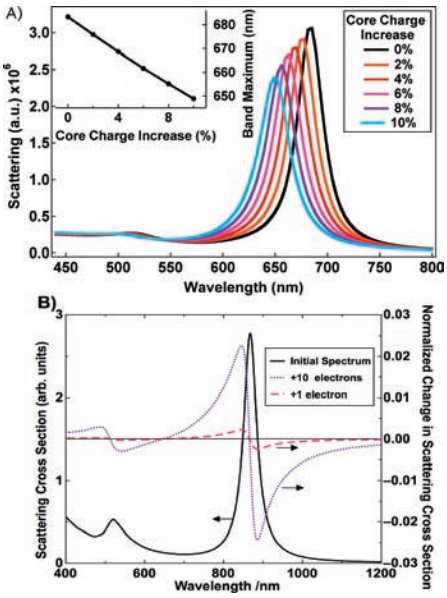

Figure 4. (A) Calculated scattered light spectra (Dipole Approximation) of charged gold nanorods, using eq 3, corresponding to the rod in Figure 2F. (B) Scattered light spectrum of a single nanorod comprising 9835 gold atoms ($a = b = 2$ nm; $c = 10$ nm) in water and the normalized change in scattered light intensity, for the injection of 1 and 10 electrons, calculated using eq 4.

The surface plasmon resonance is incredibly sensitive to the number of injected electrons. Consider a smaller gold ellipsoid with transverse semiaxes $a = b = 2$ nm and a major semiaxis with length $c = 10$ nm, for which the number of gold atoms per rod is ~9800. The injection of just one electron would yield a blue shift of <0.05 nm according to eq 2, which is beyond the resolution of current spectrometers. However, the differential change in the scattering intensity around the surface plasmon peak as a result of the blue shift can still be significant. The scattering cross section may be calculated using the Rayleigh formula, eq 3, where x is the size parameter. The calculated changes in light scattered may then be computed from eq 4 for different electron densities and are shown in Figure 4B for the cases of one and ten injected electrons. The scattered-light intensity near the longitudinal surface plasmon resonance may alter by ~0.1% for injection of a single electron and would be of order 1% for just ten injected electrons. While this detection level is beyond conventional dark-field-spectroscopy systems, these calculations raise the intriguing possibility that surface plasmon spectroscopy could provide a method for studying quantized electron transfer in the future.

$$Q_{sca} = \frac{8x^4}{3}\left|\frac{\varepsilon_{Au} - \varepsilon_m}{\varepsilon_{Au} + \frac{1-L}{L}\varepsilon_m}\right|^2 \qquad (3)$$

$$\Delta Q_{sca}(N) = \frac{Q_{sca}(N) - Q_{sca}(0)}{Q_{sca}(0)} \qquad (4)$$

In summary, we have demonstrated a method for modulating the optical properties of single gold nanorods using electrochemical charge injection. Potentials ranging from 0 to −1.6 V have been applied using a silver quasi-reference electrode, and at applied potentials ranging from −0.2 V to −1.4 V the longitudinal surface plasmon band exhibits a clear and reversible blue shift. When the plasmon band shift is large enough, color changes to a single gold nanorod can be perceived by eye. Our calculations show that surface plasmon spectroscopy provides a potential route to the optical detection of single electrons. This in turn would enable the reaction mechanisms of important redox reactions, such as hydrogen formation from water, to be studied one electron at a time, the so-called "quantum catalysis" regime.

Acknowledgment. The authors thank the ARC for funding through FF Grant 0561486. C.N. acknowledges support through a University of Melbourne International Research Scholarship. A.M.F. acknowledges support from a University of Melbourne Research Office Fellowship. The authors thank Sergey Rubanov for assistance with the FIB measurements.

Supporting Information Available: Experimental details. This material is available free of charge via the Internet at http://pubs.acs.org.

References

(1) Haruta, M. *Catal. Today* **1997**, *36*, 153. Hashmi, A. S. K.; Hutchings, G. J. *Angew. Chem., Int. Ed.* **2006**, *45*, 7896. Okumura, M.; Kitagawa, Y.; Yamaguchi, K.; Akita, T.; Tsubota, S.; Haruta, M. *Chem. Lett.* **2003**, *32*, 822.
(2) Henglein, A.; Lilie, J. *J. Phys. Chem.* **1981**, *85*, 1246. Henglein, A.; Lilie, J. *J. Am. Chem. Soc.* **1981**, *103*, 1059. Westerhausen, J.; Henglein, A.; Lilie, J. *Ber. Bunsen-Ges. Phys. Chem.* **1981**, *85*, 182.
(3) Miller, D.; Bard, A.; Mclendon, G.; Ferguson, J. *J. Am. Chem. Soc.* **1981**, *103*, 5336.
(4) Spiro, M. *Faraday Trans.* **1979**, 75. Spiro, M.; Freund, P. L. *Faraday Trans.* **1983**, *79*, 1649.
(5) Chen, S.; Murray, R. W. *J. Phys. Chem. B* **1999**, *103*, 9996. Hicks, J.; Miles, D.; Murray, R. W. *J. Am. Chem. Soc.* **2002**, *124*, 13322.
(6) Novo, C.; Funston, A. M.; Mulvaney, P. *Nat. Nanotechnol.* **2008**, *3*, 598.
(7) Klar, T. A.; Perner, M.; Grosse, S.; Von Plessen, G.; Spirkl, W.; Feldmann, J. *Phys. Rev. Lett.* **1998**, *80*, 4249.
(8) Schultz, S.; Smith, D. R.; Mock, J. J.; Schultz, D. A. *Proc. Natl. Acad. Sci. U.S.A.* **2000**, *97*, 996.
(9) Nikoobakht, B.; El-Sayed, M. A. *Chem. Mater.* **2003**, *15*, 1957. Perez-Juste, J.; Liz-Marzan, L. M.; Carnie, S.; Chan, D. Y. C.; Mulvaney, P. *Adv. Funct. Mater.* **2004**, *14*, 571.
(10) Novo, C.; Funston, A. M.; Pastoriza-Santos, I.; Liz-Marzán, L. M.; Mulvaney, P. *Angew. Chem., Int. Ed.* **2007**, *46*, 3517.
(11) Novo, C.; Mulvaney, P. *Nano Lett.* **2007**, *7*, 520.
(12) Kolb, D. M. *Angew. Chem., Int. Ed.* **2001**, *40*, 1162.
(13) Kreibig, U.; Vollmer, M. *Optical Properties of Metal Clusters*; Springer-Verlag: Berlin, Heidelberg, 1995; Vol. 25.
(14) Mulvaney, P.; Pérez-Juste, J.; Giersig, M.; Liz-Marzán, L. M.; Pecharromán, C. *Plasmonics* **2006**, *1*, 61.

JA905216H